This is an extended version of the paper presented in SEE8 conference, peer-reviewed again and approved by the JSEE editorial board.

Friction-Slip Connections for Moment Frames with Continuous Beams

Fereshteh Seifan[1], Seyed Rasoul MirGhaderi[2], and Mehdi Ghassemieh[3]*

1. Ph.D. Student, University of Tehran, Tehran, Iran,
* Corresponding Author; email: Fereshteh.saifan@gmail.com
2. Associated Professor, University of Tehran, Tehran, Iran
3. Professor, University of Tehran, Tehran, Iran

Received: 05/04/2020
Accepted: 01/09/2020

ABSTRACT

This paper presents an assessment on a friction-slip connection for moment frames with continuous beams based on the current detail. It also proposes a new configuration for rigid connections in moment frames with continuous beams, which can be developed as a friction-slip connection. In conventional moment frames, beams are placed between two adjacent columns and connected to the column flanges faces. However, in moment frames with continuous beams, two beams are continuously passed next to the column. In the existing practice for connections in these frames, two vertical connection plates placed on column flanges, and the beams are connecting to these plates via their wings. In the mentioned detail, it was assumed that the load transfers with in-plane action between connection plates and column; therefore, the design force is pure shear, and based on the design procedure, it should have been able to be developed for a friction-slip connection. However, the results showed that the out-of-plane action of RPLs could be significant; although this action provides extra capacity in moment connections, it is not desirable in friction connections due to changes in the developed forces in pretension bolts. Based on this action, a locking occurs, which changes the performance of the connection considerably. As an alternative to this detail, a new configuration is proposed in this paper, which can also be used as a friction-slip connection and provides a friction connection in moment frames with continuous beams. In new detail, by eliminating the effect of connection plate thickness, the friction joint works as expected. Thus, instead of the plastic behavior of structural elements, these friction joints can be used as an energy-dissipating system.

Keywords:
Friction-slip connection;
Bolted connection;
Continuous beams;
Moment frame

1. Introduction

Khorjini connections were a common beam to column connection in Iran for steel framing systems. In this system, two continuous beams pass next to the column, connecting to the column side using seated brackets.

Unfortunately, the seismic performance of these connections in the Manjil earthquake in 1990 was not acceptable, and many damages were observed in steel structures, especially their connections during that earthquake. The seismic behavior of these connections was studied after the earthquake, and some of its weak points were recognized [1-3]. Mirghaderi and Dehghani Renani [4] presented a new detail for moment connections in this system. In this detail, the weak points of the common Khorjini connections were eliminated, and the test results showed that this detail has an acceptable seismic performance. In the mentioned detail, the two continuous beams are connecting to the column via two vertical plates called RPL. These connection plates are welded to the column flange faces, and they also welded to beams' webs and flanges.

Figure (1) shows the view of their proposed connection; the load pass, which was determined for this connection, is shown in Figure (2).

As shown in Figure (2), where the RPLs' wings connecting to the flanges of the beams work as vertical supports for the beams, so the applied moment and shear force in the beams transfer to the column as the reaction of these vertical supports [4].

Some experimental tests were performed on three specimens with similar details of Figure (1). Moreover, some analytical studies were done [6]. The results showed that the connection with these details has enough stiffness and strength to be categorized as rigid connections.

There are some advantages in moment frames with continuous beams in comparison with conventional moment frames which make their usage attractive. Here are some of their advantages:

- An extra resistant against both gravity and seismic loads due to the continuity of beams
- Switching the panel zone from column web to beams' webs.
- Contrary to conventional moment frames, continuity plates are exposed in these connections, and this makes the welding process easier, especially in built-up box columns.
- Unlike the conventional moment connections in these connections, shear and moment forces are transferred simultaneously, and only one detail will be designed for them.

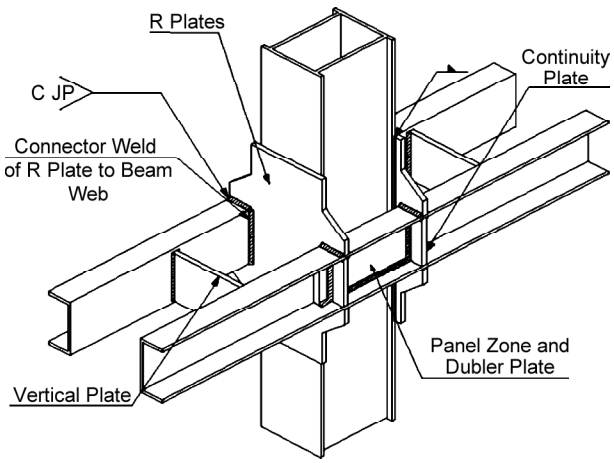

Figure 1. Rigid connection detail in moment frames with continuous beams (based on [4]).

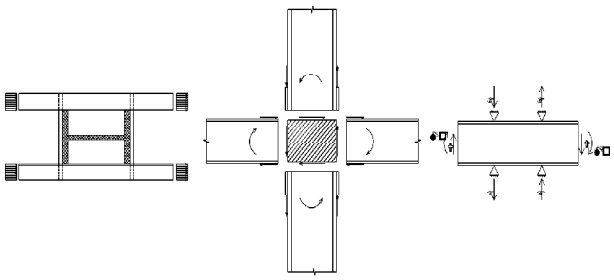

Figure 2. Load pass [5].

In conventional lateral resisting systems, usually, the ductility is provided by energy dissipation due to structural damages, such as the formation of plastic hinges in beams in moment frames and yield (or buckling) of braces in braced frames. The structural damages due to earthquakes may be unrepairable or costing a lot for being repaired, which means that after a severe earthquake, the structure might not be able to be used anymore [7]. Therefore, by developing the performance-based approach in design methods, eliminating the damage from structural elements has received more attention. In order to remove structural damages due to the energy dissipation, it is necessary to provide a replaceable source of energy dissipation for structures. Different sources of energy dissipations are used these days, and friction is one of the most common of them, which is used in many studies [8-13].

A friction assessment is done by Grondin et al. [14] for AISC about friction issues. In this assessment, the results of experiments from 1954 until 2007 were used. The results of this study say that the contact area [15], steel grade [16], and holes shapes and size [17] have not significant effect on the static friction coefficient.

Garigorian and Popov [18] assessed the energy dissipation capacity for slotted bolt connections (SBC). They assessed two types of connections with steel- steel and steel-brass contact surfaces. They showed that the steel-brass contact area provides desirable friction characteristics. They also used Belleville washers in order to reduce the change in bolts pretension load. .

Shahini et al. [9] developed a friction-slip mechanism for connections in cold-formed steel moment frames .

They used two square (SB) and circular (CB) arrangements of bolts for four beam section types and compared the results for connections with or without slip. The results showed that the circular arrangement of bolts has desirable performance and

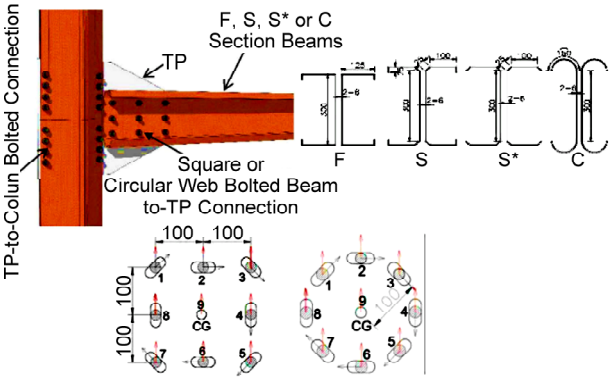

Figure 3. CFS joints with SB and CB bolting and F, S, S*, and C types of beam sections [9].

no significant contradictions observed in load distribution between bolts and the center of rotation with the design assumptions. Although the CB arrangement provided desirable performance, the SB arrangement had a delay of up to 30% in activation of group slip, which was not acceptable. They also mentioned that the slip occurrence provides more ductility and dissipate more energy (up to 75%) in comparison with bolt connections with no slippage. Figure (3) shows their assessed connection, bolts' arrangements, and beams types.

This paper presents a study on friction-slip connections for moment frames with continuous beams. Despite the conventional systems with rigid connections, in systems with friction-slip joints, the energy could be dissipated by friction, which means that there would be no structural damage in systems for this purpose.

Some assessments were performed on the friction-slip connection for current moment connection detail in these frames. The effect of pretension loads, friction coefficient, and beam stiffness in comparison with the stiffness of RPL are considered; unlike the expectations, the mentioned detail did not provide a pleasant friction performance because of the out-of-plane action of RPLs, so an alternative connection is proposed. Results of the rigid-welded connection with the new proposed configuration under cyclic load are compared with the results of the existing detail. After assuring the similarity of their behavior, the friction-slip connection with the new configuration is assessed. The effect of the pretension load, friction coefficient, and design moment is studied for this detail. As it was expected, the results showed that this new proposed connection has excellent and acceptable friction performance. It has considerable energy dissipation capacity in comparison with the corresponding rigid connection.

2. Finite Element Model

2.1. Verification

This study is focused on two subjects, friction and moment frames with continuous beams; therefore, the analytical models' verification is done in two parts. Both verification models are with solid parts in ABAQUS [19].

A rigid connection for moment frames with continuous beams is modeled based on the second specimen in [4]. The parameters of materials are based on the coupon test for the mentioned experimental specimen, and Figure (4) shows the considered material behavior diagram in software; the hardening of materials is considered combined with the half-cycle type. Lateral supports for beams and boundary conditions are similar to the mentioned experimental specimen. The SAC protocol, based on Figure (5), is applied on top of the column.

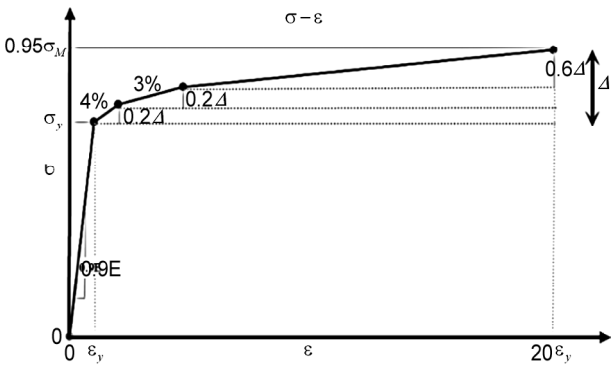

Figure 4. The considered shape of the material behavior chart in the ABAQUS.

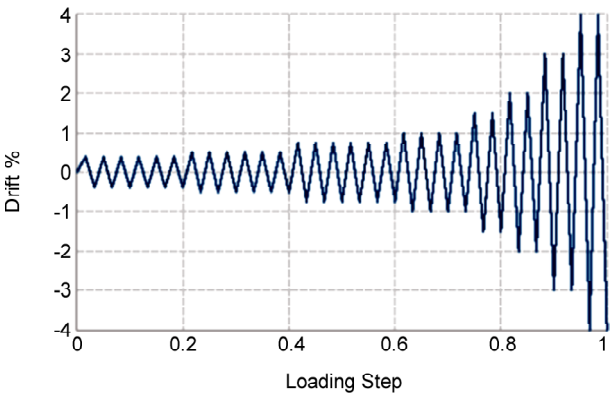

Figure 5. SAC loading protocol [20].

A self-center friction connection is modeled based on the second specimen in [21]. The boundary conditions are defined similar to the mentioned specimen, and the lateral load was applied to the beam's end. The material is defined in the elastic form in ABAQUS because no plastic behavior was observed in the experimental result. The bolts are modeled with the solid parts. The bolts' rods, heads, nuts, and washers are merged. The pretension load is applied with the "Bolt Load" option of ABAQUS in the first step. The comparison between the analytical and experimental results for both models is shown in Figure (6).

2.2. Assessed Models Specifications

All models are assessed in ABAQUS with 3D, solid, deformable parts. The elements mesh types are C3D8R and C3D6, and the material definition is similar to which explained in section 3.1. The other modeling parameters are as follow:

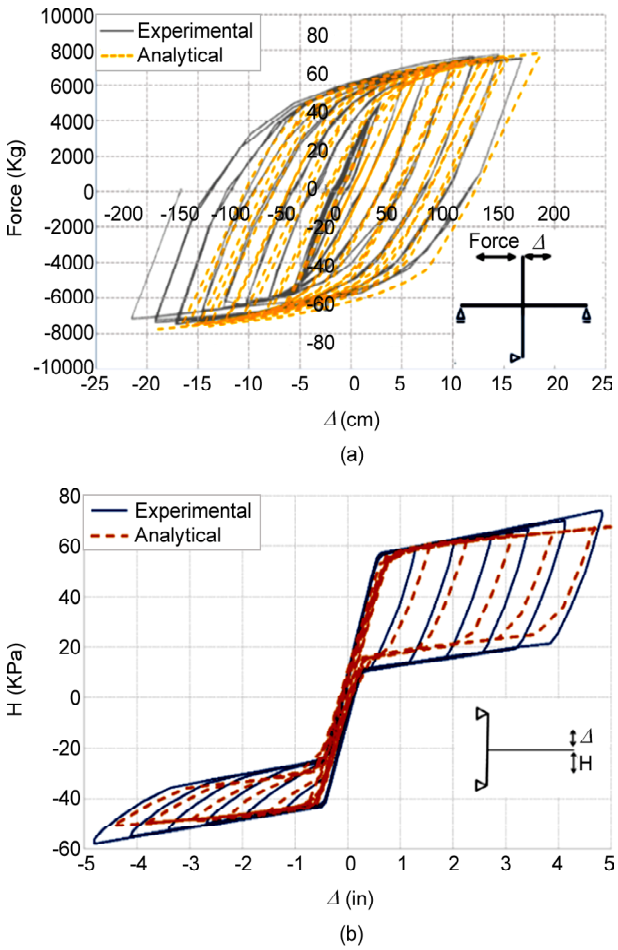

Figure 6. The verification of analytical results of the (a) Rigid-welded connection based on [4], and (b) Self-center friction connection based on [21].

2.2.1. Steps and Loads

In rigid-welded models, only one step, Lateral step, with general static type, is defined after the initial step. The lateral displacement is applied to the top of the column at this step.

Bolted connection models are similar to rigid ones with an extra dynamic implicit type step, Bolt load step, before the Lateral step. The pretension loads of bolts are applied in the Bolt load step with the "Bolt load" option of ABAQUS, and in a quasi-static way to eliminate the effects of load appliance speed.

2.2.2. Boundary Conditions

A rigid plate is tied to beams' and column's webs at the end of them. Boundary conditions and external lateral loads are applied to the center of these plates' external faces. Vertical plates are coupling the beam sections and providing lateral support for them. Figure (7) shows boundary conditions for all assessed models; connection plates are not shown in this figure.

2.2.3. Interactions

In welded connections, the fillet welds are modeled, and their elements are tied to structural parts; groove welds are modeled with the tie interaction. In bolted connections in addition to existing welds, two interactions from contact type are defined: the Normal interaction, and the Friction interaction. Table (1) shows the specification of each interaction. Table (2) shows the corresponding area of each interaction.

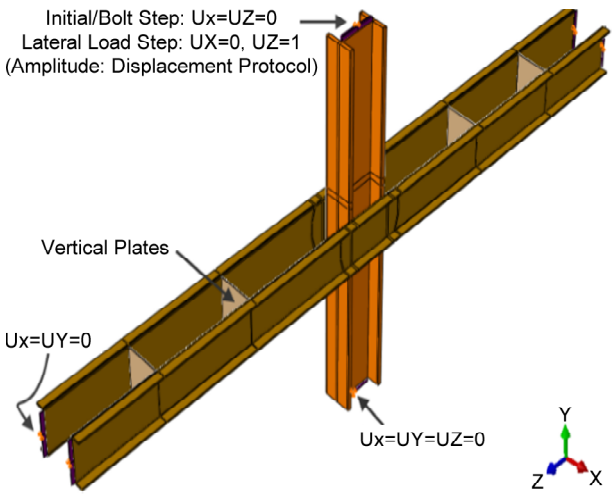

Figure 7. Boundary conditions in all assessed models.

3. Friction-Slip Connection with the Current Detail

A three-story prototype building is designed with moment frames with continuous beams; the configuration of this prototype building is similar to one of the SAC's [22]. A sub-assemblage of this designed building is assessed analytically with ABAQUS. Some parametric studies are done on connection plates, beams size, and friction conditions.

As it is shown in Figure (2), the connection with current practice is designed for pure shear between column and R-Plate; therefore, in order to have a friction-slip connection for this detail, the welds which connect R-Plates to the column are replaced by pretension bolts. Standard holes are considered on R-Plates and slotted holes on the column. The bolts are designed for shear at which the slip occurrence is assumed. In friction-slip connections, the slip occurrence is prior to the formation of plastic hinges in beams. Therefore, the demand for the friction connection is smaller than the demand in the corresponding rigid connection. The assessed friction connection is shown in Figure (8). The friction parameters are based on [12].

Eight models are assessed, their specifications are shown in Tables (3) to (5), and the parameters

Table 1. Contact interaction types for bolted models.

Interaction Name	Behavior and Formulation	
	Normal Behavior	Tangential Behavior
Normal Interaction	Hard Contact	Friction—Frictionless
Friction Interaction	Hard Contact	Friction—Penalty—Isotropic (With Friction Coefficient Based on [12])

Table 2. Contact interaction area for bolted models.

Interaction Name	Contact Area
Normal Interaction	- Bolts' Rods and Holes - Bolts' Nuts with their Corresponding Contact Surfaces - Beam and Connection Plate Contact Area in the New Practice
Friction Interaction	- Bolts' Heads with their Corresponding Contact Surfaces - Connection Plate with the Column Flanges in the Existing Practice - Connection Plates with each other in the New Practice

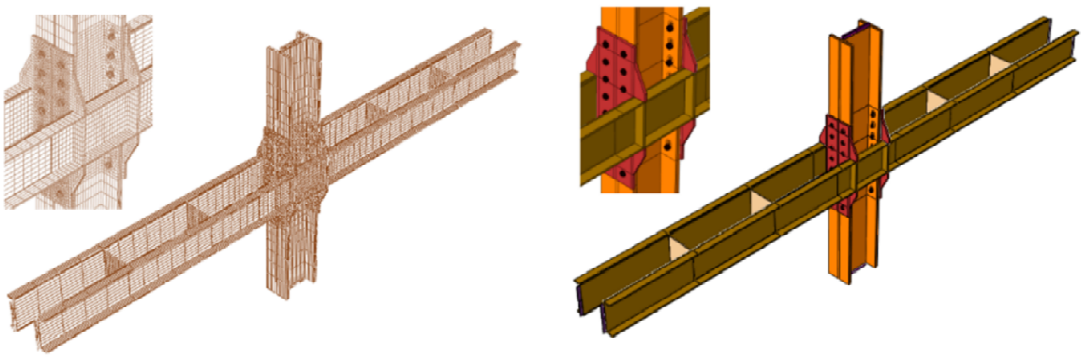

Figure 8. View of the assessed friction-slip connection with current detail.

Table 3. Structural elements' geometric parameters.

Element	Shape	Geometric Parameters (mm)						
		Section				Length		
Beam	Channel (Double Section)	U_1—web 460×10- flanges 120×20				9140		
		U_2—web 440×20- flanges 150×30				9140		
Column	H-Shape	Web 500×30- flanges 400×50				3960		
RPL	Based on Figure 9	Group	L1	L2	L3	L4	L5	L6
		1	130	450	500	500	260	80
		2	160	450	500	650	450	200
Doubler Plate Thickness (mm)		Group 1				10		
		Group 2				20		

Table 4. Main models' specifications.

Group	Model	Beam	RPL |Thickness (mm)	Number of Bolts at Each Side (n_b)	Pretension Load (T_b)-kN	μ
Group1	Model1	$2U_1$	30	16	407	0.4
	Model 2	$2U_1$	50	16	407	0.4
	Model 3	$2U_1$	10	16	407	0.4
Group2	Model 4	$2U_2$	35	18	340	0.4
	Model 5	$2U_2$	50	18	340	0.4
	Model 6	$2U_2$	20	18	340	0.4

Table 5. Other models' specifications.

Model	Pretension Load (T_b)-kN	μ
Model 1a	203.5	0.8
Model 1b	814	0.2

for RPLs are based on Figure (9).

First of all, models 1, 1a, and 1b are assessed to assure the correctness of design procedure assumptions; because of the equality of the friction force of the connection design, which is corresponding to the connection shear, it was expected that the results are similar. Contrary to expectations, the results showed that the frictional behavior of these three models is different. The normal force between column and R-Plate, which is initially provided by the pretension load of bolts ($n_b \times T_b$), does not remain constant during displacement appliance. As presented in Figure (10), by increasing the amount of this load, the motion threshold friction force increases with the ratio of μ, so the slip occurrence is postponed. The locking occurs between R-Plates and column, which restricts the amount of slip, and as a result of that, the plastic behavior of structural elements is probable. By increasing the bolts' pretension load, the change in Normal force

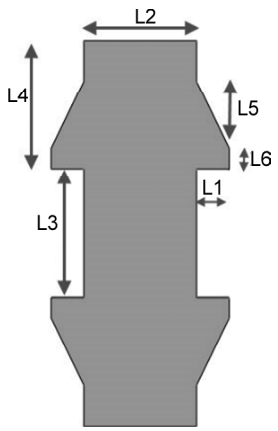

Figure 9. R-Plate shape and geometric parameters.

decreases.

The above results show that in the existing detail since the Normal force changes from its initial amount, the friction force is not calculated based on $\sum_{i=1}^{n_b} T_{bi} \times \mu$, and this otherness from the design assumptions changes the behavior of the friction connection in an unpleasant way. In order to find the reason for this contradiction, the rest of the models, defined in Table (4), are assessed.

The Normal and Friction forces of these models in the contact area are shown in Figures (11) and (12).

In models 4-6 (group 2) the increase in the R-Plate thickness leads to an increase in the Normal force in the contact area. In the model with 20 mm thickness, this increase is about 4.7%; in the model with 35 mm thickness, it is about 5.7%, and in the model with 50 mm thickness, this increase is about 5.9%,

Figure 12. Unlike the models 4-6, no considerable change is observed in Normal force of models 1 and 2, since no slippage occurred in model 3, it is excluded from the assessment of friction parameters.

Figure (13) shows the Von Mises stress distribution in webs of the column and beams (in the panel zone) for models of group 1 (1-3).

In models 1 and 2, the increase in R-Plate thickness leads to an increase in the stress of beams' and column's webs. In model 3, no slippage observed, so the distribution of stress is similar to rigid connections (Figure 13).

The Von-Mises stress and Equivalent plastic strain distribution in webs of the column and beams (in the panel zone) for models of group 2 (4-6) are presented in Figures (14) and (15), respectively.

Based on the results for models 4-6, an increase in R-Plate thickness will increase the potential of panel zone formation in the web of the column. In

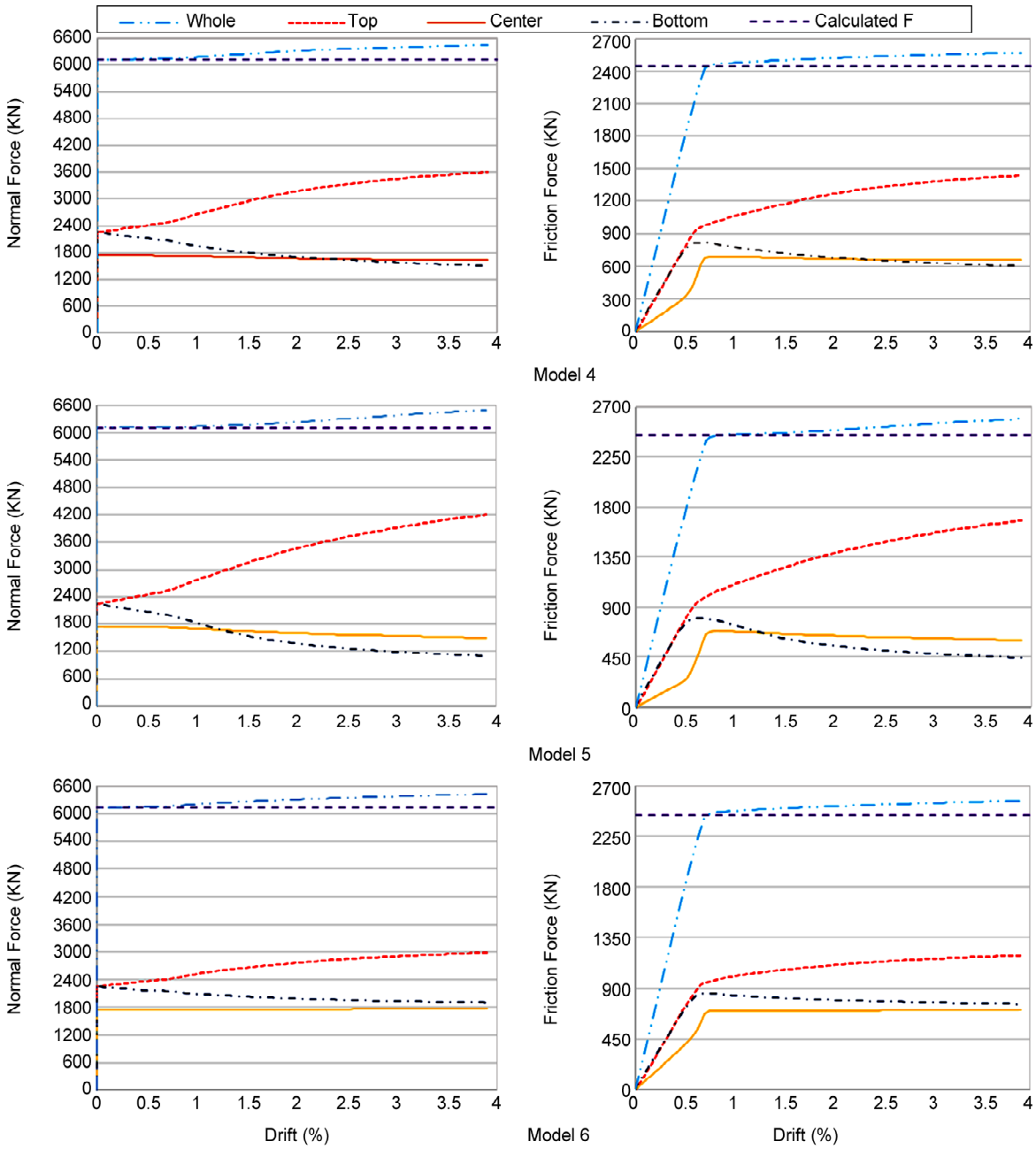

Figure 10. The Normal and Friction force in whole, top, center, and bottom of the left contact area based on drift.

the model 6 (thin R-Plate) the stress level in the web of the column is lower than in beams; but in the model 4 the stress level in the web of the column is higher than in beams, and in the model 5 (thick R-Plate) not only the stress in the web of the column is higher but also the plastic behavior is observed in this area (Figures 14 and 15).

3.1. Moment Assessment in Friction Connection

In order to find the reason for observed contradictions, an assessment on connection moment for all models is done. Figure (16) presents the assumed free diagram for the connection. Based on this diagram, the moment relations are presented in Equation (1).

$$\begin{cases} M_{beam} = \dfrac{L_b}{2} \times (|B_1 + B_2| + |B_3 + B_4|) \\ M_{Col} = \dfrac{h_c}{2} \times (|C_b| + |C_t|) \\ M_{connection} = \dfrac{d_c}{2} \times (|F_{left}| + |F_{right}|) \end{cases} \xrightarrow[F_{friction} = N_b \times T_b \times \mu]{it\ is\ expected\ that} M_{beam} = M_{Col} = M_{connection} = F_{friction} \times d_c \quad (1)$$

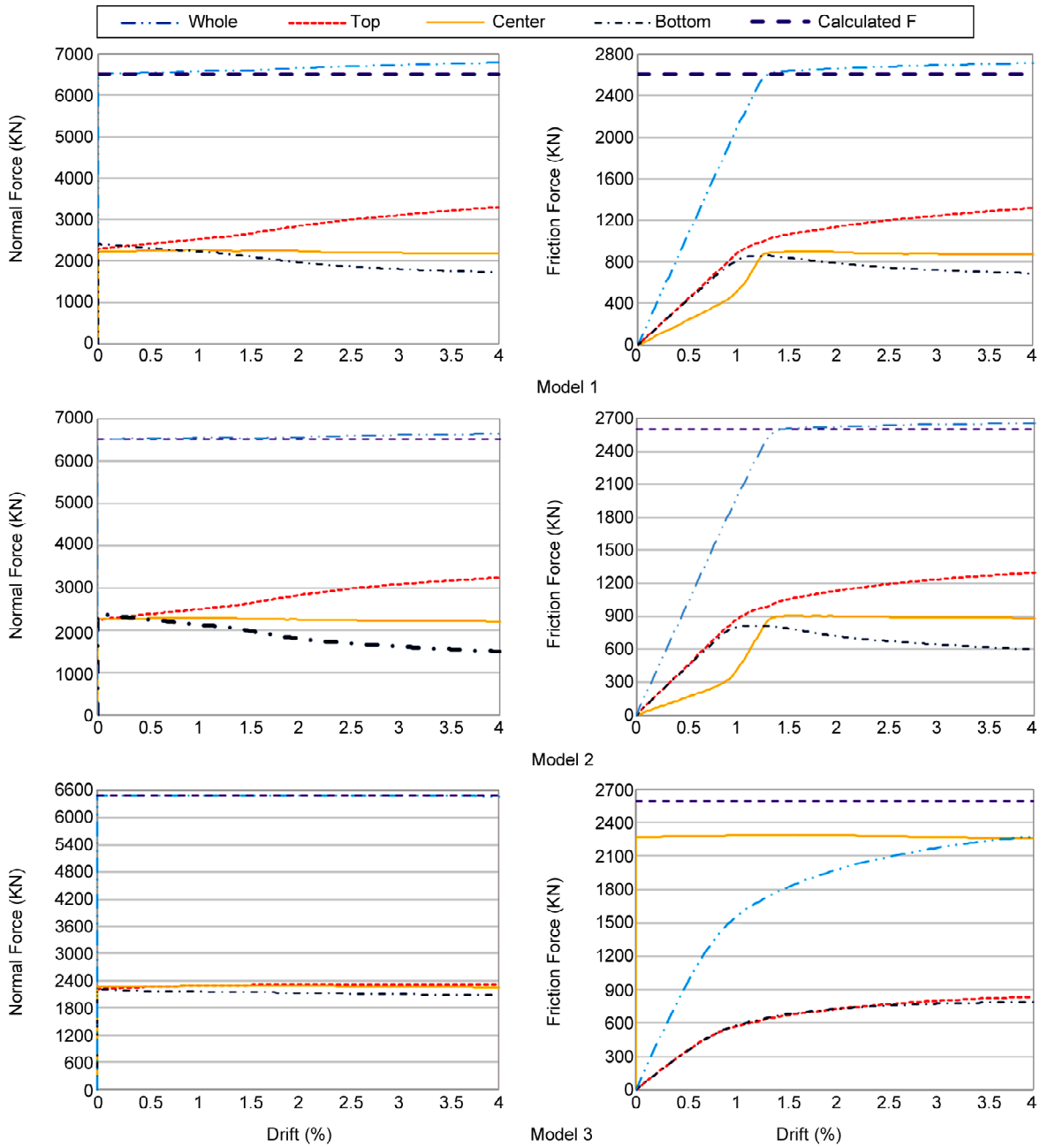

Figure 11. Normal and Friction force due to pretension bolts in whole, top, center, and bottom part of the contact area for models of group 1 based on the drift.

Equation (1) is not satisfied for all models; some Normal components are observed in the top and bottom of the contact area between RPLs, and the column. Thus the actual free diagram of the connection based on the results and observations is presented in Figure (17). The modified moment relation based on this free diagram is presented in Equation (2).

$$M_{beam} = M_{Col} = M_{connection} + M_{out\ of\ plane}\left[= \alpha(|F_4 + F_2| + |F_3 + F_1|) \times \frac{h'}{2}\right] \quad (2)$$

The results and summary of assessments are shown in Table (6). As it is shown, in each group by increasing the R-Plate thickness, the amount of α, and the difference between occurred and expected slip are increased.

3.2. Observations

- In models 4, 5 and 6 (group 2) the increase in the R-Plate thickness leads to increase in the Normal force in the contact area; in model with 20 mm thickness this increase is about 4.7%, in the model with 35 mm thickness it is about 5.7%,

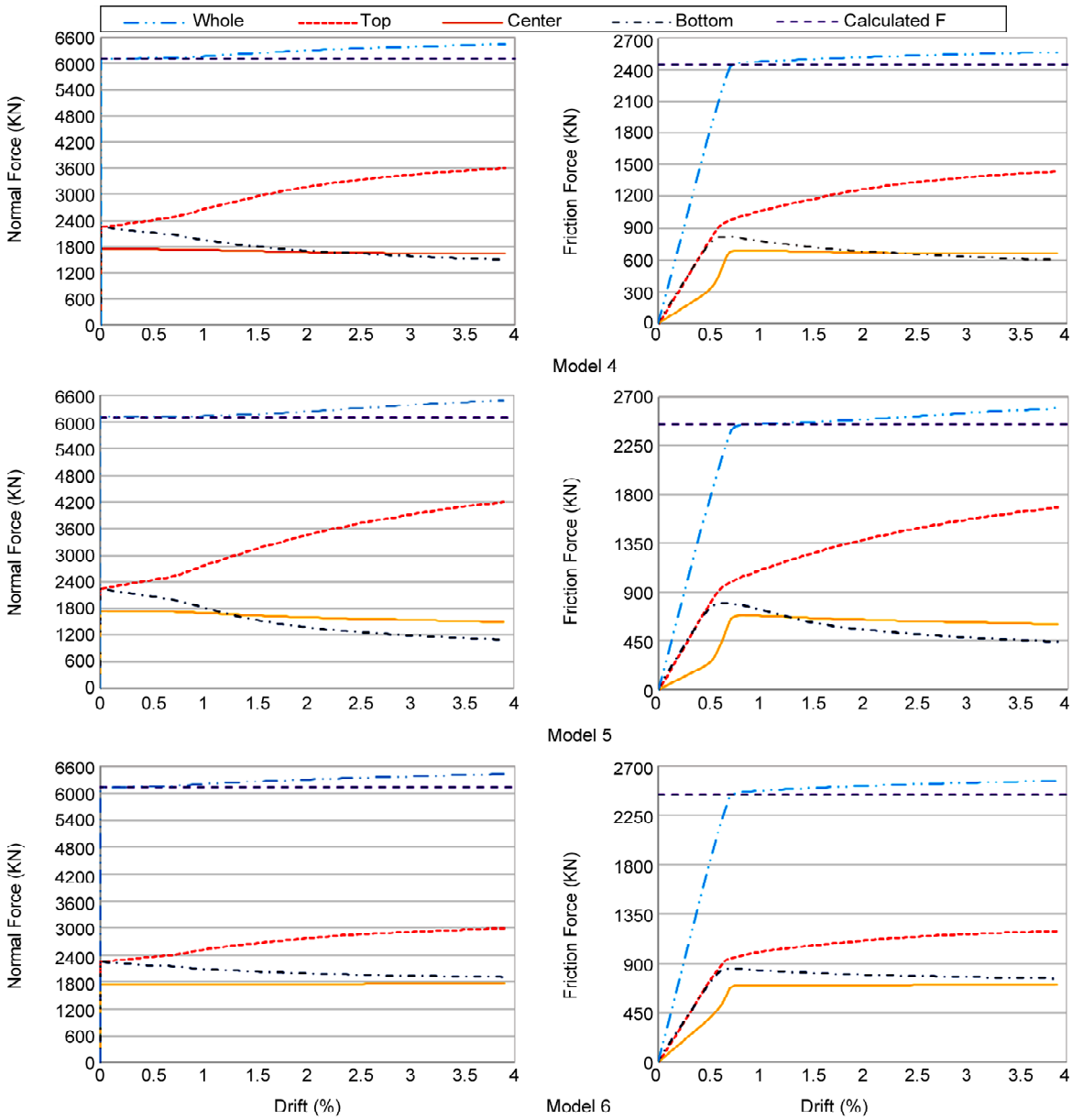

Figure 12. Normal and Friction force due to pretension bolts in whole, top, center, and bottom part of the contact area for models of group 2 based on the drift.

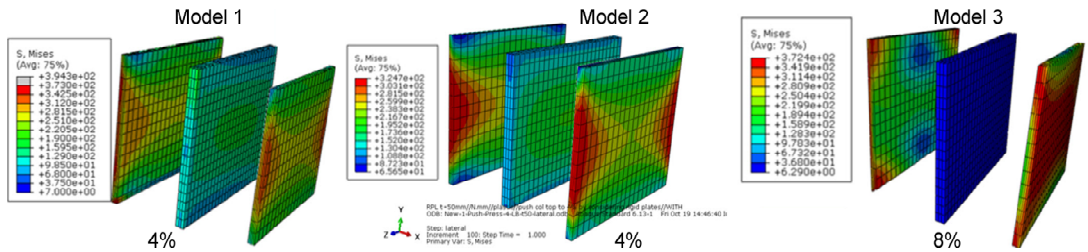

Figure 13. Mises distribution in webs of the column and beams for pushover analysis up to 4 or 8%, for models 1 to 3.

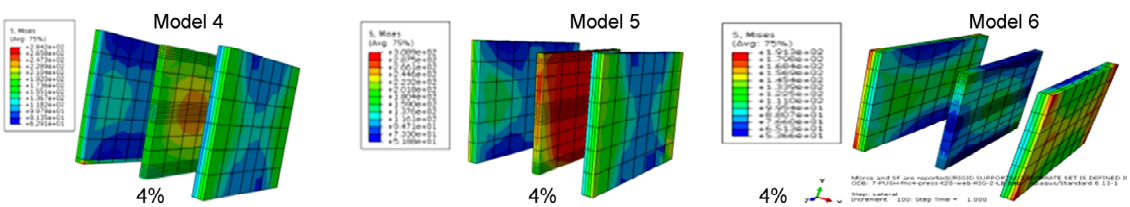

Figure 14. Mises distribution in webs of the column and beams for pushover analysis up to 4% for models 4 to 6.

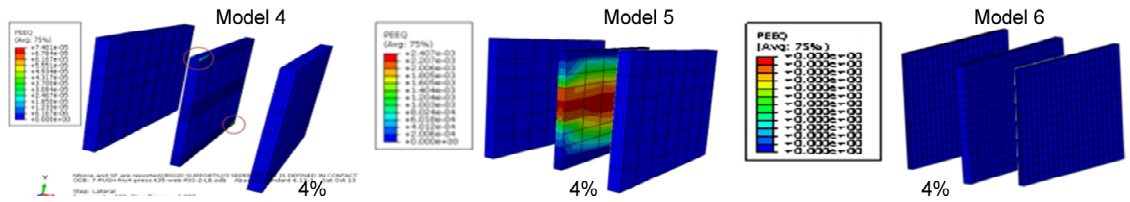

Figure 15. Equivalent plastic strain distribution in webs of the column and beams for pushover analysis up to 4% for models 4 to 6.

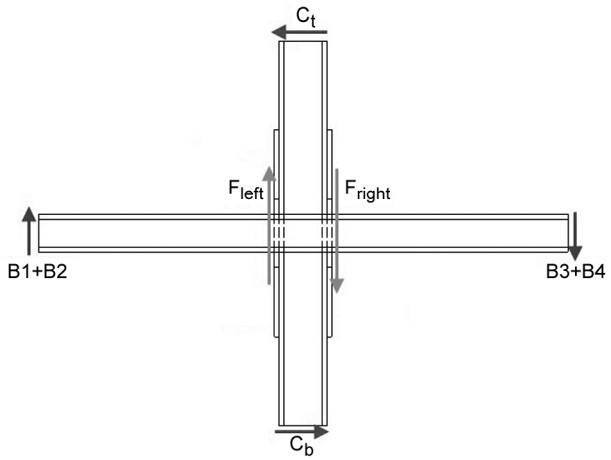

Figure 16. The assumed free diagram of the connection.

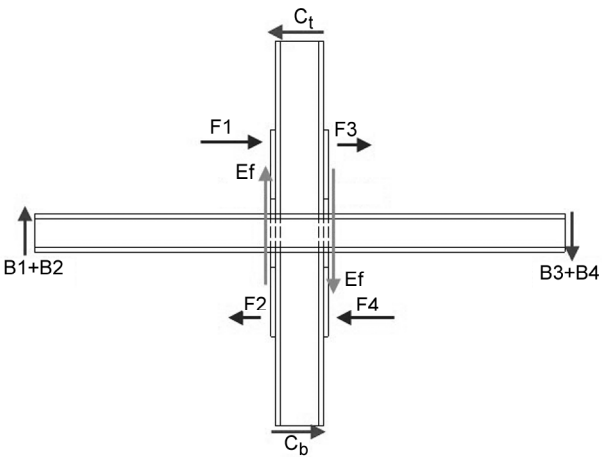

Figure 17. The actual free diagram of the connection.

Table 6. Summary of results for six assessed models.

		Group 1			Group 2		
Model		3	1	2	6	4	5
R-Plate Thickness (mm)		10	30	50	20	35	50
Drift at Which Slip Started		-	1.3	1.33	0.7	0.7	0.7
Slip	Expected Slip (mm)	-	16.2	16.02	19.2	19.2	19.2
	Observed Slip (mm)	-	12.25	6.09	17.96	17.88	17.6
Change in the Total Normal Force		-	4%	0.4%	4.7%	5.4%	5.9%
Panel zone		Beams' Webs	Beams' Webs	Beams' Webs	Beams' Webs	Column's Web	Column's Web
α*		0.29	0.71	0.83	0.68	0.7	0.74

* α : Assumed correction factor for considering the out-of-plane action of RPLs.

and in the model with 50 mm thickness, this in crease is about 5.9% (Figure 12)

- Figure (12). Unlike models 4-6, no considerable change is observed in the Normal force of models 1 and 2 (since no slippage occurred in the model 3; it is excluded from the assessment of friction parameters) (Figure 11).

  Based on the results for the models 4, 5, and 6, an increase in R-Plate thickness will increase the potential of panel zone formation in the column's web. In the model 6 (thinner R-Plate) the stress level in column web is lower than beams', but in the model 4 the stress level in column's web is higher than beams' and in the model 5 (thicker R-Plate) not only the stress in column's web is higher but also the plastic behavior is observed in this area (Figures 13 and 14). In models 1 and 2, the increase in R-Plate thickness leads to an increase in the stress of beams' and the column's webs, but in comparison with group 2 this change is small, and the demand in beams' webs is higher than columns. In model 3, no slippage observed, so the distribution of stress is similar to rigid connections Figure (13).
- Occurred slips in models are lower than expected, especially in models 1 and 2 (no slippage observed in model 3).
- By increasing the R-Plate thickness, more extensive areas of connections will become plastic; in model 5, a large part of the flanges and the webs of the beams are in plastic form.

4. New Configuration for Connections

In order to eliminate the out-of-plane action of connection plates, the new configuration is proposed in Figure (18). The results show that the rigid connection with this configuration (Figure 18-a) works similarly to the rigid connection with the existing detail. As it is shown in Figure (18), in this detail, the webs of the beams are connected to the column's flanges via one or two circular connection plates (these plates can be part of a circle; based on the required number of bolts or welds length) at each side of the connection, PL1 (and PL2). In rigid-welded connections, the beams' webs and flanges and also the column flanges are connected to PL1 (Figure 18-a) and in bolted connections, the two connection plates, PL1 and PL2, are connecting by the circular arrangement of bolts (Figure 18-b); PL1 is welded to the beam's web and flanges, and PL2 is welded to the column's flanges. For executive consideration, PL2 should be the same size or smaller than PL1.

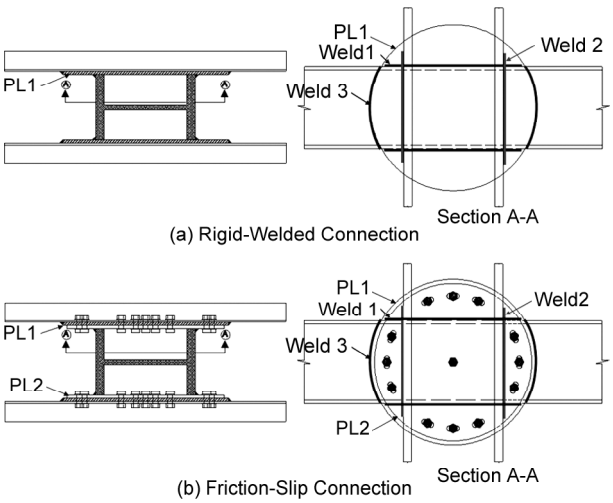

Figure 18. View of the new proposed.

4.1. Verification of the Rigid-Welded Connection

The comparison of the new and the existing detail is made for rigid-welded connections. The structural elements of the existing detail are similar to model 1 presented in Table (3), with the 30 mm RPL and 15 mm doubler plate (Figure 19). The view of the assessed welded connection with the new configuration is shown in Figure (20).

In connection with the new practice, the column and beams are based on Table (3), and other geometric parameters of elements are shown in Table (7). The connection plate is strengthening the panel zone, so there is no need for a doubler plate in this specimen.

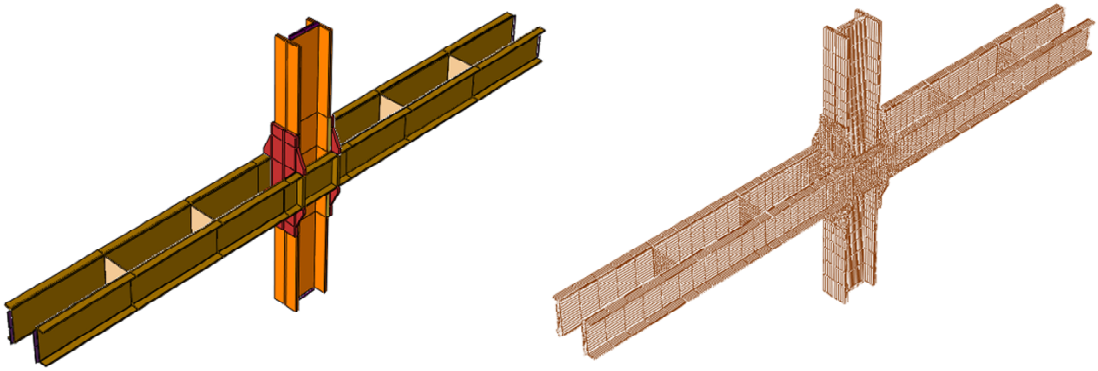

Figure 19. The new detail of the rigid welded connection with finite element mesh.

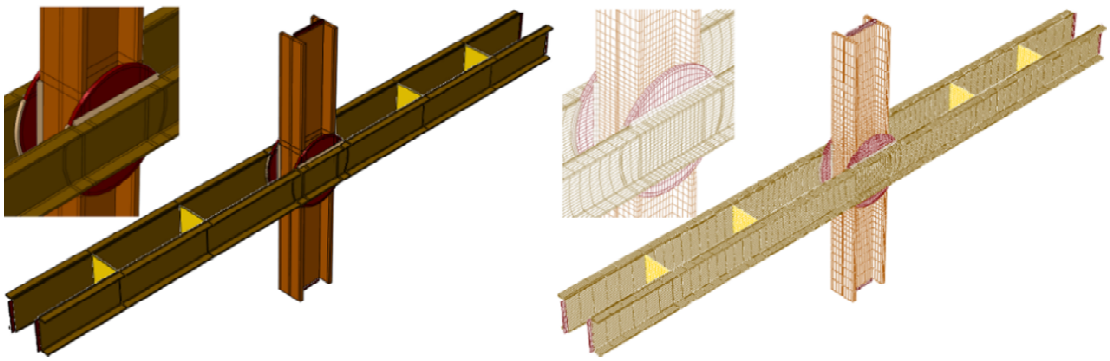

Figure 20. The new detail of the rigid welded connection with finite element mesh.

The equivalent plastic distribution in both models is similar (Figure 21), and plastic hinges are formed in beams.

As it is shown in Figure (22), the stress distribution in beams and column webs in the connection area show that in both details, the potential of the panel zone formation is in the webs of the beams.

The hysteresis responses of the welded connection with both existing and new configurations, which are almost the same, are shown in Figure (23).

Table 7. Geometric parameters of structural elements for rigid welded connection with the new practice.

Connection Plate	Shape	Diameter (mm)	Thickness (mm)
PL1	Whole Circle	1000	30

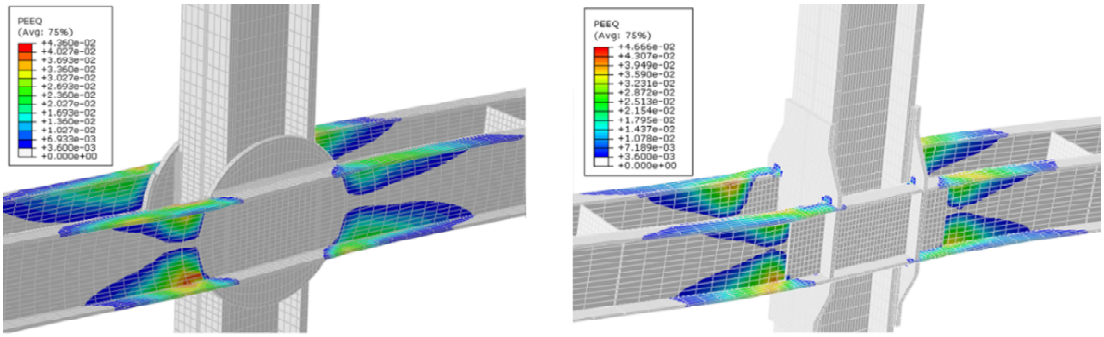

(a) The New Practice (b) The Existing Practice

Figure 21. The equivalent plastic strain for rigid-welded connections for pushover analysis up to 8% drift.

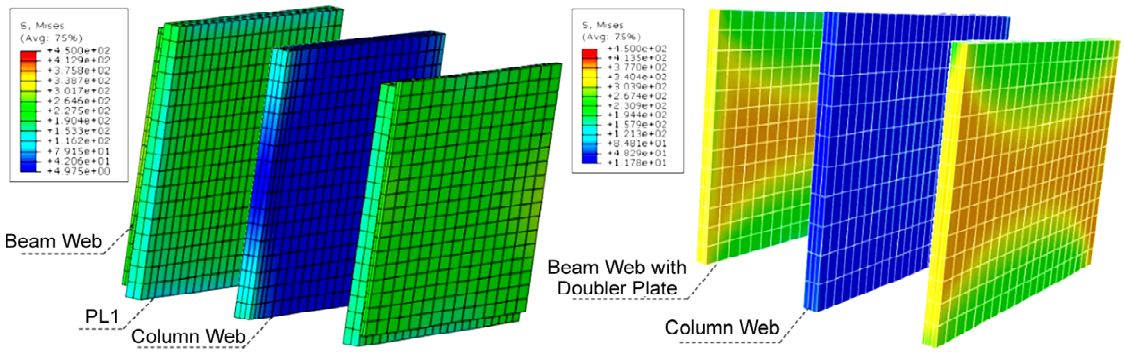

(a) The Existing Detail (b) The New Practice

Figure 22. Mises distribution in webs of the column and beams for pushover analysis up to 8%.

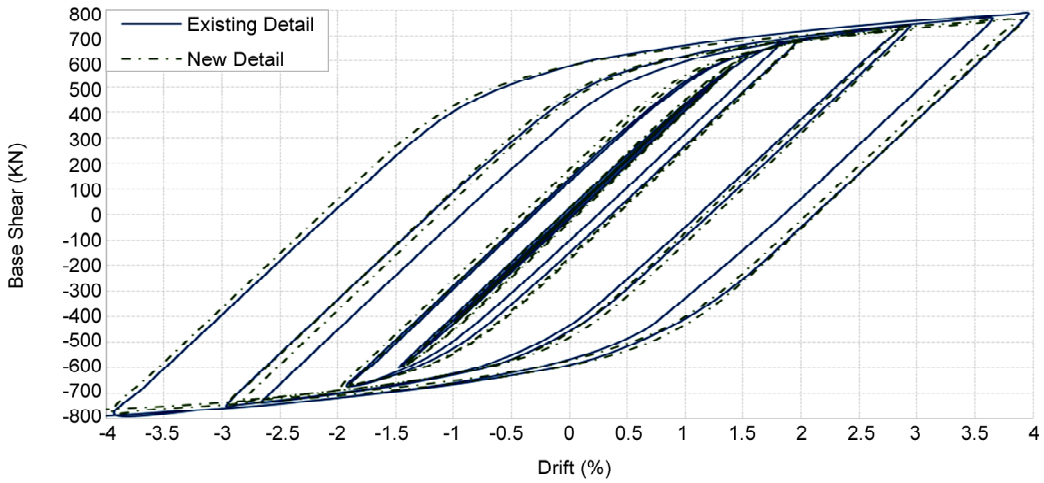

Figure 23. Comparison between the base shear-drift responses of the existing and the new detail of the rigid welded connection in moment frames with continuous beams

4.2. Friction-Slip Connection

After assuring the similar results of the new rigid-welded connection with the current one in moment frames with continuous beams, the bolted connection with slotted holes is assessed. The connection design can be divided into five parts:

- The connection between PL1 and PL2 (bolts);
- The connection between PL1 and beam (weld1 and weld3);
- The connection between PL2 and column (weld2),;
- The connection plates' thickness;
- Shear control of panel zone.

4.2.1. Bolt's Design

The pretension bolts provide moment and shear resistance of the joint via friction performance. The size and the pretension load of bolts will be designed for connection moment, $M_{connection/slip}$, Equation (3); the sufficiency of this design will be checked by considering the effect of shear force in reducing the moment capacity of the connection. Two simplified assumptions are considered here, the equal contribution of bolts to the design shear and simultaneous slip of them despite the shear effects. Figure (24) shows the connection plates and bolts circular arrangements.

$$M_{connection/slip} = \max(\beta M_{connection}, 2M_{frame\ design}) \quad (3)$$

4.2.2. Connection Plates

Connection plates and weld lines are shown in Figure (25). Weld1 will transfer the connection moment, $M_{connection/slip}$, from beam to PL1, and Weld3 will transfer the shear, $V_{des/half/slip}$ (Equation 4); therefore, they will be designed for moment and shear, respectively. Weld2 will be designed for the connection moment and a $\frac{n''}{n'}$ portion of the connection shear based on Figure (26).

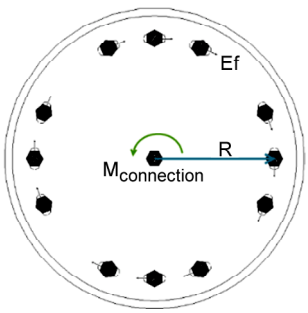

Figure 24. The connection plates and bolts- friction force due to their pretension load.

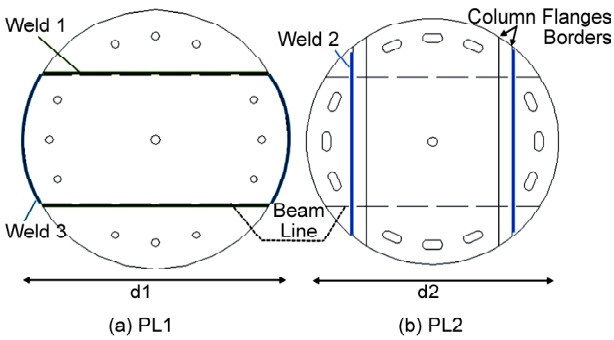

Figure 25. Geometric details of the connection plates.

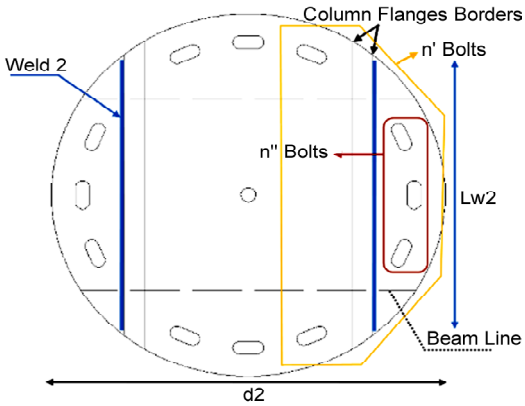

Figure 26. The geometric details of PL2.

$$V_{des/half/slip} = \max(\beta V_{des/half}, V_{frame\ design}) \quad (4)$$

In addition to the welds sizes criterion, the shear demand on connection plates plays a role in determining their thickness. Based on the $V_{des/half/slip}$, yield and rupture of plates should be controlled.

4.2.3. Panel Zone

In friction connections, it is assumed that the slippage will occur prior to plastic hinge formation in beams, so there is no need to control the panel zone; unless in high drifts which bolts will reach to the holes' edges. However, in rigid-welded connections, the control of the panel zone is necessary. Similar to the existing detail for rigid-welded connections in moment frames with continuous beams, the potential of panel zone formation is in webs of the beams here. Weld1 and weld2 are specifying the panel zone area (Fgure 27).

The panel zone thickness will be calculated by the summation of the beam web and the connection plate thicknesses.

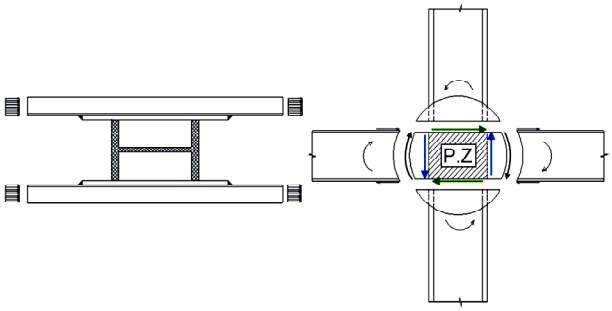

Figure 27. The Connection free diagram and the panel zone in the new proposed rigid-welded connection.

4.2.4. Friction- Slip Connection Models

The friction-slip connection based on the new configuration is designed and assessed analytically. Figure (28) shows the view of the assessed models. Table (8) shows the specification of models; all bolts are from the A490 type.

Beams and column sections are based on Table (3). In Table (8):

- t_1 and t_2 are the thickness of PL1 and PL2, respectively. d_1 and d_2 are shown in Figure (25).
- N is the number of bolts in the radius R from the center of plates.
- T_b is the pretension load of each bolt, and μ is the considered friction coefficient. The actual amount for μ is 0.4 [12].

5. Results

As expected, in all models, the Normal forces on both sides of the connections are the same. These forces match with the calculations based on the multiplication of the number of bolts to their pre-tension load.

Figure (29) shows the developed moment between connection plates due to the friction performance of pretension bolts for the right side of connections for a cyclic analysis up to drift 4%. The whole connection moment capacity can be calculated based on the summation of connection moments at both sides.

The stable hysteresis responses of the connections say that the friction works perfectly. As long as the design moment is constant, change in and have no effects on the results, which means that there is no unexpected source of moment capacity in the connection; Figure (30) also confirms this subject. The whole moment capacities of the connections are compared with the moment based on the reaction forces of beams in Figure (30). Based on Figure (30), it can be concluded that, along the entire beam, the moment is less than in connections. Since the connection moment capacity is less than the plastic moment of beams, the beams will stay elastic in all models.

Figure (31) shows the base shear results for all friction models:

After initiating the slippage, the amount of base shear is constant, and no plastic behavior is seen in

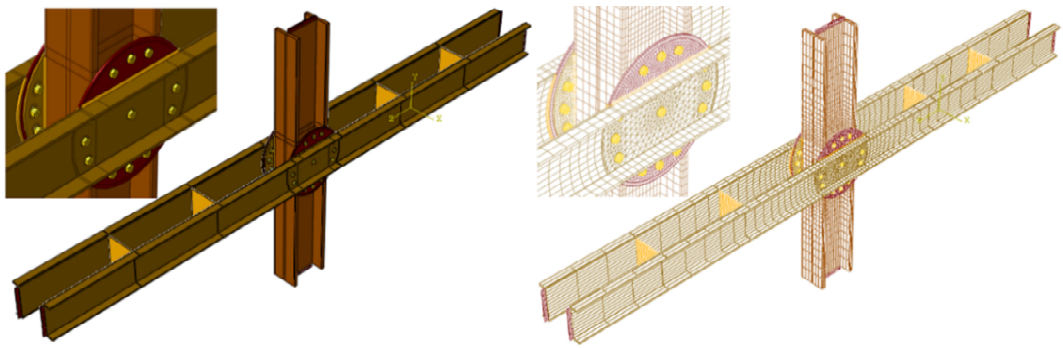

Figure 28. New proposed friction connection with the finite element mesh.

Table 8. The specifications of friction models with the new configuration.

Beam	β*	Model	d_1 (mm)	t_1 (mm)	d_2 (mm)	t_2 (mm)	N	Bolt Size	R (mm)	μ	Tb (kN)	ψ**
U_1	0.7	1	1000	15	950	15	12	M30	400	0.4	484	0.69
		2	1000	15	950	15	12	M30	400	0.8	242	--
	0.55	3	1000	15	950	15	12	M30	400	0.4	389	0.55
		4	1000	15	950	15	12	M30	400	0.8	144.5	--

** $T_b = \psi F_u A_{nb}$; A_{nb} and F_u are the nominal area and the ultimate strength of the bolts, respectively.

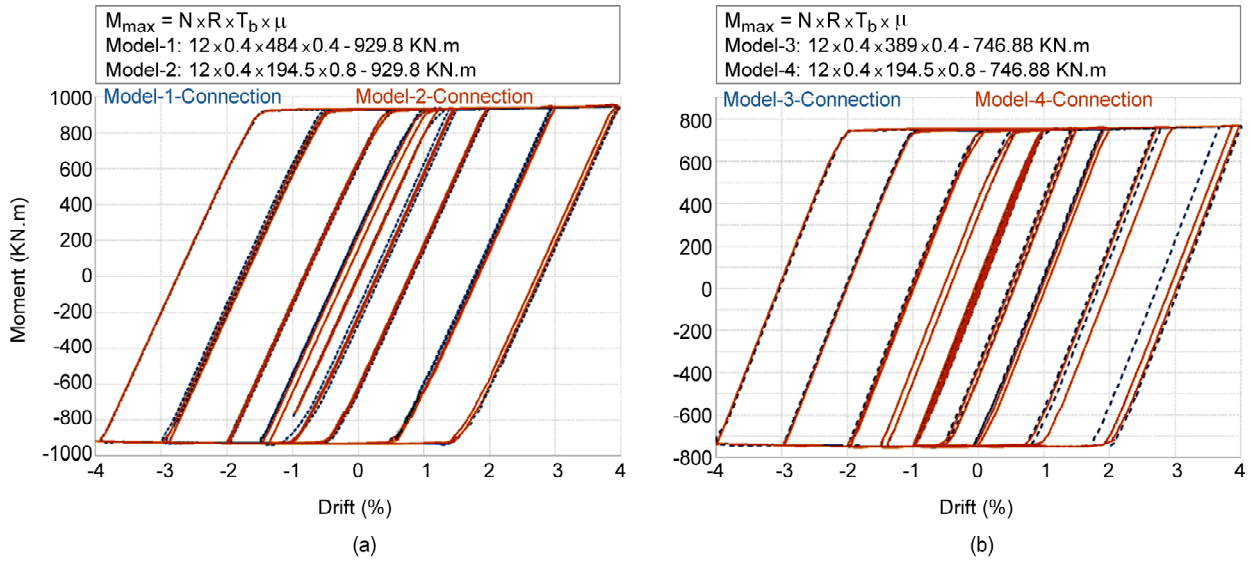

Figure 29. The connection moment for all models for a cyclic displacement applied up to 4% drift.

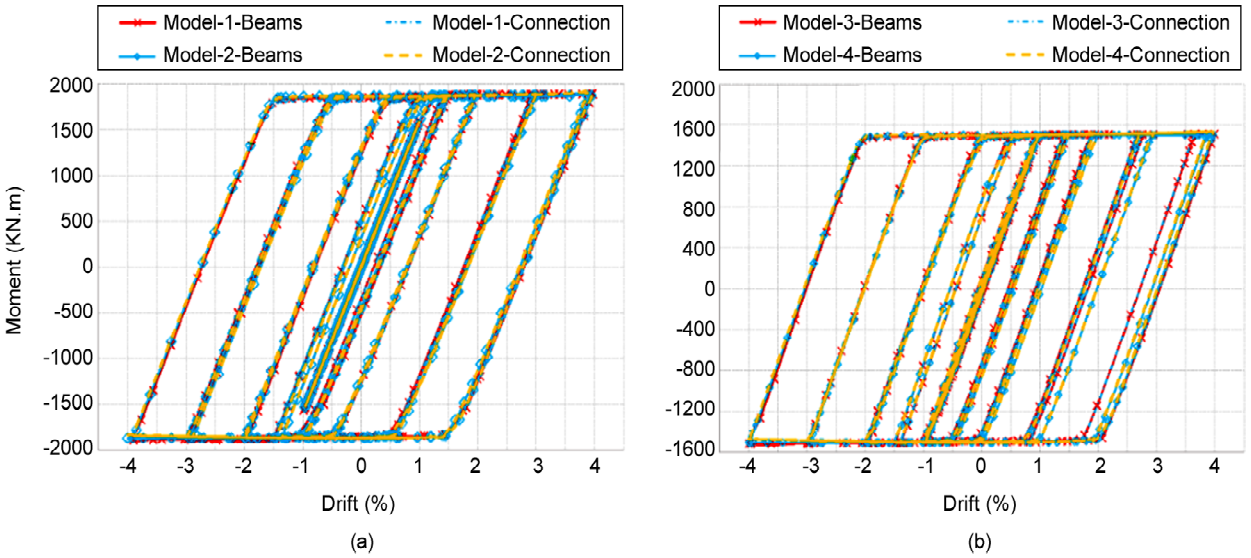

Figure 30. The comparison between connection moment capacity and the beam moment in all models for a cyclic displacement applied up to 4% drift.

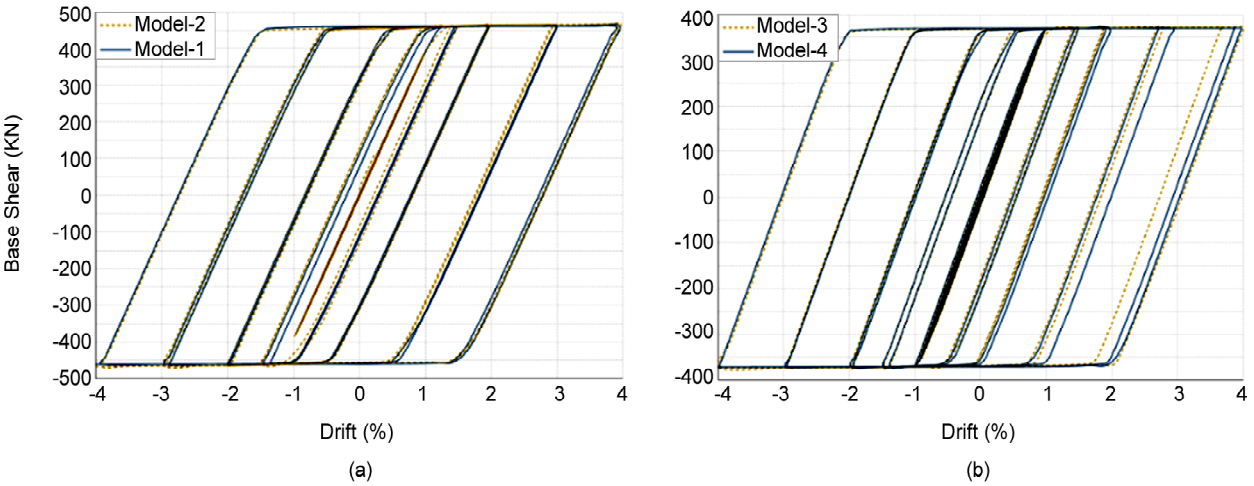

Figure 31. The comparison of base shear-drift results for models 1 and 2 for a cyclic displacement applied up to 4% drift.

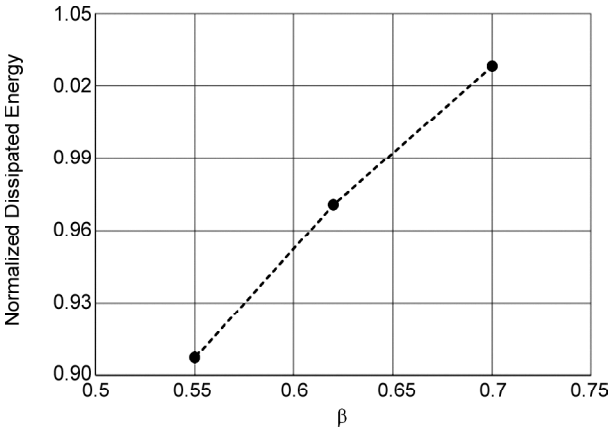

Figure 32. Normalized dissipated energy of models based on the corresponding welded connections.

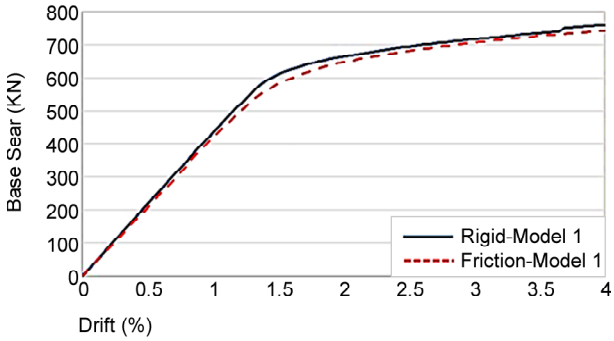

Figure 33. Base shear-drift response for model 1 with friction-slip connection and rigid-welded connection.

structural elements. This behavior continues until the amount of occurred slippage reaches to the maximum allowed amount based on the size of holes. To avoid this contact, using long slotted holes and providing enough space for the slip is necessary.

For pushover analysis up to 4% drift, the maximum difference between the bolt's slippage amount with each other and with the theoretical amount is less than 2%, which means that the bolts reach the slip threshold simultaneously.

The amount of energy dissipation of models 1 and 3, introduced in Table (8), and one extra model; a model with U_1 beams, and $\beta = 0.62$, are compared with the corresponding rigid-welded connections based on the area of the hysteresis curves. The results show that by increasing the amount of β, the energy dissipation amount increases (Figure 32).

6. Conclusion

- In models with the current detail of connection in moment frames with continuous beams:
  - The effect of beam stiffness (size) in comparison with R-Plate's is vital in determining the amount of occurred slip versus expected. slip In group 2, the beams are stiffer, so the slip occurs sooner, and its amount is nearer to the expected amount. By increasing the R-Plates' stiffness (thickness), the occurred slip is reduced. In other words, a minimum stiffness is needed for a beam to be able to move R-Plate on a col umn flange. On the other hand, a minimum stiffness is needed for R-Plate to provide enough stiffness for connection to improve the force level of connection to the slip threshold force. Moreover, the point is that none of these minimums and their effects are mentioned in the design procedure.
  - Unlike group2, in group 1, by increasing the R-Plate thickness, no considerable change is observed in the Normal force, and also the occurred slippage is small. These observations lead to an assumption that the Normal force is almost constant because the behavior of these connections is so close to rigid connections. The similarity between base shear- drift responses of model 1 with friction and rigid welded connections confirm the above assumption (Figure 33).
  - Inequality of the connection moment with beams and column moment say that there is another parameter in providing the connection moment capacity; the results show that the out of plane action of R-Plates is affective in this extra capacity of the connection. By increasing the R-Plate thickness, the portion of this component will increase. α in Table (6) refers to this effect.
- In models with the new proposed configuration of connection (in moment frames with continuous beams):
  - The new proposed configuration with the rigid-welded connection works similar to a rigid connection with the existing detail.
  - The results show that an assumption of simultaneous slippage of bolts is acceptable with an approximation of less than 2%.
  - After initiating the slippage in friction connections with the new proposed configuration, the base shear and connection moment level remains constant with an acceptable approximation, which means that the circular slippage

works correctly and no plasticity will occur in the structure. This behavior continues until the bolts reach the holes edge and a locking occur, which leads to an increase in the base shear amount, and as a result of that, the plastic behavior will be observed. Using long slotted holes will prepare enough space for slippage before locking.

- The results show that as long as the design moment is constant, the change in pretension load of bolts or the friction coefficient does not change the connection performance.
- By increasing the "β" parameter, the energy dissipation value increases.

References

1. Karami, R. (1992) *Study of Rigidity Khorjini Connections*. Sharif University of Technology, Department of Civil Engineering.
2. Asghari, S. (1999) *Experimental Study of Khorjini Connections*. Amirkabir University of Technology, Department of Civil and Environmental Engineering.
3. Sadeghian, P. (1999) *Analytical Study of Khorjini Connections*. Sharif University of Technology, Department of Civil Engineering.
4. Mirghaderi, S. and Dehghani Renani, M. (2008) The rigid seismic connection of continuous beams to column. *Journal of Constructional Steel Research*, **64**, 1516-1529.
5. Dehghani Renani, M. and Mirghaderi, R. (2006) The new details of rigid connection. *Proceedings of First European Conference on Earthquake Engineering,* Geneva.
6. Dehghani, M. (2001) *Analytical and Experimental Studies of Khorjini Beam to Column Connections and New Detail of Rigid Connection*. School of Civil Engineering, University of Tehran.
7. Chancellor, N.B., Eatherton, M.R., Roke D.A., and Akbas, T. (2014) Self- Centering seismic lateral force resisting systems: high performance structures for the city of tomorrow. *Buildings*, 520-548.
8. Christopoulos, C. Tremblay, R., Kim, H., and Lacerte, M. (2008) Self-centering energy dissipative bracing system for the seismic resistance of structures: Development and validation. *Journal of Structural Engineering*, **134**(1), 96-107.
9. Shahini, M., Sabbagh, A.B., Davisdon P., and Mirghaderi, R. (2019) Development of cold-formed steel moment- resisting connections with bolting friction- slip mechanism for seismic applications. *Thin- Walled Structures*, **141**, 217-231.
10. Roke, D.A. Sause, R., Ricles, J.M., and Chancellor, N.B. (2010) *Damage-Free Seismic-Resistant Self-Centering Concentrically-Braced Frames*. ATLSS Report No. 10-09, Bethlehem.
11. Ricles, J. Sause, R. Garlock, M., and Zhao, C. (2001) "Posttensioned seismic-resistant connections for steel frames. *Journal of Structural Engineering*, **127**(2), 113-121.
12. Wolski, M.E. (2006) *Experimental Evaluation of a Bottom Flange Friction Device for a Self Centering Seismic Moment Resistant Frame with Post-Tensioned Steel Moment Connections*, M.S. Thesis, Dept. of Civil and Environmental Eng., Lehigh University, Bethlehem, PA.
13. Nabid, N., Hajirasouliha, I., and Petkovski, M. (2019) Adaptive low computational cost optimisation method for Performance- based seismic design of friction dampers. *Engineering Structures*, **198**.
14. Grondin, G., Jin, M., and Josi, G. (2008) Slip critical bolted connections- a reliability analysis for design at ultimate limit state. University of Alberta.
15. Nester, E. (1966) Influence of variation of the contact area upon the slip resistance of a bolted joint. Lehigh University.
16. Kuperus, A. (1996) *The Ratio between the Slip Factor of Fe 52 and Fe 37*. Delf University of Technology.
17. Allan, R. and Fisher, J. (1968) Bolted joints

with oversized and slotted holes. *Journal of the Structural Division*, **94**, 2061-2080.

18. Garigorian, C.E. and Popov, E.P. (1994) *Energy Dissipation with Slotted Bolted Connections*. College of Engineering University of California at Berkeley.

19. S. Inc (2012) *ABAQUS Analysis User's Manual Version 6.12-1*.

20. Seismic Provisions for Structural Steel Buildings, Illinois (2016) American Institute of Steel Construction (AISC).

21. Wolski, M., Ricles, J.M., and Sause, A.R. (2009) Experimental study of a self-centering beam-column connection with bottom flange friction device. *Journal of Structural Engineering*, **135**(5), 479-488.

22. Akshay Gupta, H.K. (1999) *Seismic Demands for Performance Evaluation of Steel Moment Resisting Frame Structures*. Department of civil and Environmental Engineering Stanford University, Stanford.